Short Report

Low Temperature Synthesis of CdSiO₃ Nanostructures

Leonardo P. Santana, Erick S. de Almeida, Jones L. Soares and Flavio M. Vichi*

Instituto de Química, Universidade de São Paulo, Av. Prof. Lineu Prestes, 748, Bloco 3T, Sala 325, 05508-900 São Paulo-SP, Brazil

Descreve-se a síntese de nanoestruturas de $CdSiO_3$ cristalino como fase única a 580 °C; ao que sabemos, esta é a mais baixa temperatura de formação observada até o presente para este composto. A formação da fase desejada ocorre somente a partir de de 580 °C, já que a 570 °C os picos de difração estão deslocados para menores ângulos em relação ao padrão JCPDS 85-0310. A fonte de silício influencia diretamente a morfologia do material: Na_2SiO_3 leva à formação de nanopartículas na forma de agulhas, ao passo que sílica mesostruturada de alta área superficial leva a partículas coralóides. A difratometria de raios X em baixo ângulo mostra que o caráter mesoestruturado da sílica precursora não se mantém no $CdSiO_3$ resultante. A microscopia eletrônica de varredura sugere que, neste caso, haja uma transição da morfologia esférica do precursor para a morfologia em forma de agulhas do material obtido a partir de Na_2SiO_3. A área superficial do precursor de sílica utilizado tem influência direta na formação de $CdSiO_3$, pois o uso de sílica comercial de menor área superficial não resulta no produto desejado.

We report the synthesis of single-phase, crystalline $CdSiO_3$ nanostructures at 580 °C; to the best of our knowledge, this is the lowest temperature at which this material is reported to form. The desired phase does not form below 580 °C, since the diffraction peaks are shifted to lower angles in the material treated at 570 °C when compared to JDPDS Card No. 85-0310. The source of silicon has strong influence on the product morphology: Na_2SiO_3 yields single-phase $CdSiO_3$ in needle-shaped nanostructures, while high surface area mesostructured SiO_2 yields coralloid-shaped particles. Low angle X-ray diffractometry reveals that the mesostructured nature of the silica precursor is not maintained in the resulting $CdSiO_3$. Scanning electron microscopy suggests that in this case a transition occurs between the spherical morphology of the precursor and the needle-shape morphology of the material prepared from Na_2SiO_3. The surface area of the silica precursor has a strong influence in the reaction, since the use of commercial silica with a lower surface area does not yield the desired product.

Keywords: cadmium metasilicate, morphology control, molten precursor method

Introduction

In recent years, compounds that exhibit the property of long lasting phosphorescence (LLP) have become of great interest. This phenomenon is observed when a compound is capable of absorbing visible and UV light, storing the energy and releasing it as visible light, resulting in a long lasting afterglow in the dark.[1] These materials have a wide range of applications, such as emergency lighting and road signs, and medicinal applications are possible in principle.[2,3] The phenomenon has been known since ancient times and a good example is the Stone of Bologna, studied by Galileo himself, which shows a yellow-orange afterglow when exposed to sunlight due to the presence of BaS impurities.[4-6]

The silicate family is an attractive class of materials for almost any application due to its interesting properties such as water and chemical resistance, visible light transparency, color variety upon doping and especially ease of preparation.[7-10] Cadmium metasilicate, $CdSiO_3$, is a promising material due to its low dimensional structure, which consists of a one-dimensional chain of edge-sharing SiO_4 tetrahedral units with metal cations compensating the negative charge.[11,12] This type of structure permits easy insertion of ions into the host lattice which can be used to tune the excitation energy storage and subsequent emission at room temperature.[13] In the last decade, a series of long-lasting phosphors based on $CdSiO_3$ have

*e-mail: fmvichi@iq.usp.br

been prepared, with different colors based on the dopant. Examples include $CdSiO_3$:Y, La, Gd, Lu (indigo),[14] $CdSiO_3$:Sm^{3+} (pink),[15] $CdSiO_3$:Pr^{3+} (reddish-orange),[16] and $CdSiO_3$:Dy^{3+} (white).[17] Also, different colors have been obtained through the combination of suitable dopants.[18] The so-called conventional solid state route for preparing $CdSiO_3$ consists of thoroughly mixing the precursors (generally $CdCO_3$, SiO_2 and the dopant oxide) followed by heating this mixture above 1000 °C for at least 3 h.[15,18,19] This method has some disadvantages, such as high energy consumption and inhomogeneous mixing, resulting in irregularly shaped and aggregated particles.[20] There have been some recent successful attempts at preparing $CdSiO_3$ at lower temperatures using different precursors. The material has been obtained at 900 °C for 60 min via a sol-gel method[21] and $CdSiO_3$:Mn^{2+} has been grown on Si(100) substrates via a vapor-phase deposition process at 700 °C for 60 min.[22] In this case, nanowire bundles attached to the substrate are obtained, a morphology different from that normally observed when the conventional high-temperature solid state route is employed.

In this contribution we report the synthesis of single-phase $CdSiO_3$ using a molten reactant route in which one of the reactants is in the molten state, since $CdCl_2$ has a melting point of 564 °C. Molten salt synthesis is a simple, versatile and cost-effective strategy to prepare high-purity, single crystalline phase materials at lower temperatures and shorter reaction times when compared to conventional solid state methods.[23,24] Above the melting point of the salt, the precursor molecules/units diffuse rapidly through the highly ionic medium, resulting in nucleation and growth of the desired phase. This step is extremely sensitive to reaction conditions such as salt species, amount of salt, reaction temperature and duration.[25] Once the reaction is complete, any excess salt can be easily removed by washing with deionized water.

Using this approach, we have obtained $CdSiO_3$ at 580 °C for 60 min using $CdCl_2$ and two different Si sources: commercial sodium metasilicate, Na_2SiO_3, and a high surface area mesostructured SiO_2 obtained by a surfactant-template synthesis. Our synthesis conditions, 580 °C for 60 min represent, to the best of our knowledge, the lowest temperature and the shortest time at which pure, single-phase crystalline $CdSiO_3$ is reported to form.

Experimental

Synthesis of mesostructured silica

Mesostructured silica was prepared as follows: 0.6 g of hexadecyltrimethylammonium bromide (CTAB, Sigma) was added to a mixture of 2.0 mL of 2 mol L^{-1} NaOH and 180 mL of water at 80 °C. After 30 min, 3.0 mL of tetraethyl orthosilicate (TEOS, Aldrich) were added dropwise under fast stirring and the resulting suspension was kept at 80 °C for 2 h. The suspension was allowed to cool to room temperature and was filtered and thoroughly washed until the pH of the filtrate was between 6.5 and 7. The material was dried overnight at 80 °C and then heated at 550 °C for 3 h to eliminate excess CTAB. This mesostructured silica shows a narrow pore size distribution with an average pore diameter of 4.6 nm, a pore volume of 0.96 cm^3 g^{-1} and a surface area of 1139 m^2 g^{-1}.

Synthesis of CdSiO₃ nanoparticles

All reagents were used as received. $CdSiO_3$ powders were prepared using $CdCl_2$ (Merck) as the cadmium source and two different sources of silicon: commercial sodium metasilicate, Na_2SiO_3 (Vetec) and a mesostructured silica obtained by the surfactant-templating route described above. The reagents (1:1 Cd:Si molar ratio) were mixed and ground for 10 min in an agate mortar using small amounts of ethanol to aid in mixing. The resulting thick slurry was dried overnight at 60 °C, after which it was ground again. This dry mixture was heated at 580 °C for 60 min using a 5 °C min^{-1} ramp, and was allowed to cool overnight inside the oven. One experiment using $CdCl_2$ and Na_2SiO_3 was also done at 570 °C. The resulting $CdSiO_3$ powders were thoroughly washed in deionized water until no Cd^{2+} could be detected by addition of S^{2-}(aq) to the filtrate and no Cl^- could be detected by addition of Ag^+(aq). For clarity, the material prepared using sodium silicate will be called SS-$CdSiO_3$ and the material prepared using mesostructured silica will be called MS-$CdSiO_3$.

The $CdSiO_3$ nanostructures and the mesostructured SiO_2 precursor were characterized by X-ray diffraction (XRD, Shimadzu Maxima XRD-7000, CuK_α, 15.418 nm, 2° *per* min), scanning electron microscopy (SEM, JEOL JSM-7401 FESEM, operating in SEI mode at 5 kV), transmission electron microscopy (TEM, Zeiss CTEM 902, operating at 80 kV), and focused ion beam microscopy (FIB, FEI Nova 200 Dual Beam SEM/FIB, 5 kV). The BET surface areas given as Supplementary Information (Figure S2) were determined by nitrogen adsorption (Quantachrome Nova 1000e Surface Area Analyzer).

Results and Discussion

Figure 1 shows the XRD patterns of $CdSiO_3$ (JCPDS Card 35-0810) (a), SS-$CdSiO_3$ (b) and MS-$CdSiO_3$ (c).
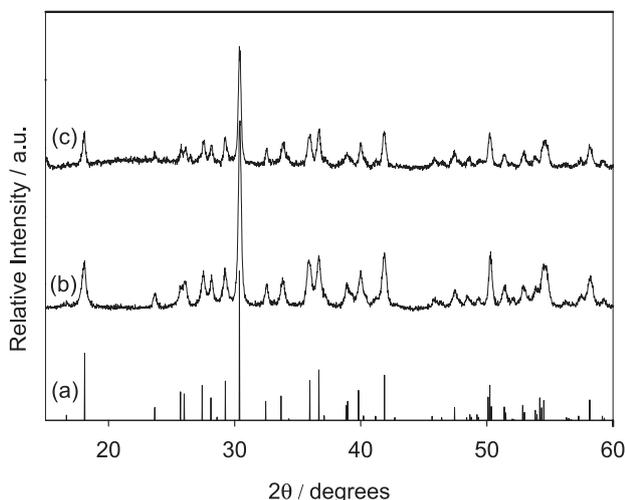
Figure 1. XRD patterns for (a) JCPDS Card No. 35-0810; b) SS-CdSiO$_3$; c) MS-CdSiO$_3$.

A comparison of the diffractograms with JCPDS Card No. 35-0810 (Figure 1a) confirms that SS-CdSiO$_3$ consists of pure, single-phase CdSiO$_3$, whose structure is expected to be similar to that of pseudowollastonite, CaSiO$_3$.[10] We can also see that MS-CdSiO$_3$ is slightly less crystalline and exhibits a halo between 2θ = 20 and 30°. Sodium metasilicate is sometimes also described as Na$_2$O·SiO$_2$, and sodium oxide can react with silica to form the silicate structure which, in the presence of molten CdCl$_2$, forms the desired product. The attack of SiO$_2$ by Na$_2$O prior to CdSiO$_3$ formation probably leads to higher crystallinity. The XRD patterns of the materials obtained from CdCl$_2$ and Na$_2$SiO at 570 °C for 1 and 5 h (Figure S1) are almost identical to that obtained at 580 °C for 1 h, but are shifted by 0.15° to higher values of 2θ (for example, the strongest peak occurs at 2θ = 30.40° and 30.55° for the samples heated at 580 and 570 °C respectively). This indicates that, although the material forms at 570 °C, that is, soon after the melting of CdCl$_2$, the ordering of the structure is not complete below 580 °C.

The use of a high surface area mesostructured silica also yields CdSiO$_3$, although with a somewhat lower crystallinity, as evidenced by the broader, less intense XRD peaks. The broad halo between 2θ = 20 and 30° indicates that the reaction is not complete, and some amorphous SiO$_2$ remains. However, low-angle X-ray diffraction (Figure 2) shows that the mesostructure of silica is lost upon the partial conversion to CdSiO$_3$. At the reaction temperature, we expect SiO$_2$ to be less reactive than the Na$_2$O present in the metasilicate precursor. In this case the precursor surface area does play a fundamental role, allowing a more effective contact between the molten CdCl$_2$ and the Si source. When we used commercial fused silica with a lower surface area (354 m^2 g^{-1}) as the Si source, no CdSiO$_3$ was formed at 580 °C for 1 h.
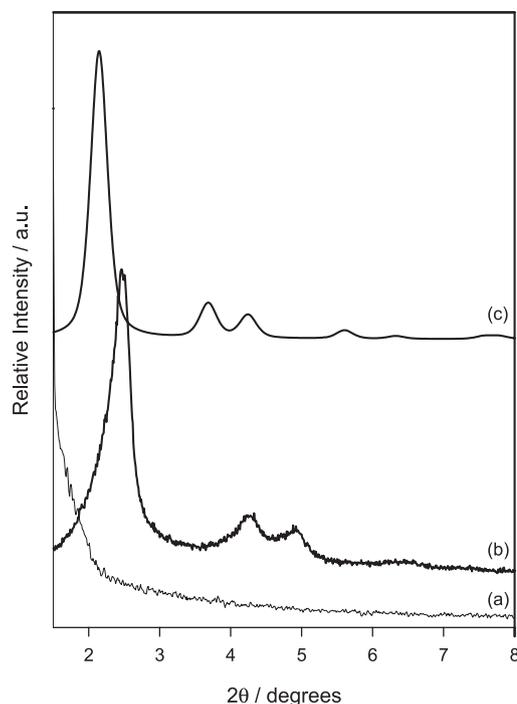

Figure 2. Low angle X-ray diffractograms of MS-CdSiO$_3$ (a) and of the mesostructured silica used in this work (b). For comparison, the JCPDS card for MCM-41 silica is also shown (c).

The SEM results are shown in Figure 3. The images show that there is a significant influence of the Si source on the morphology of the resulting product which, in
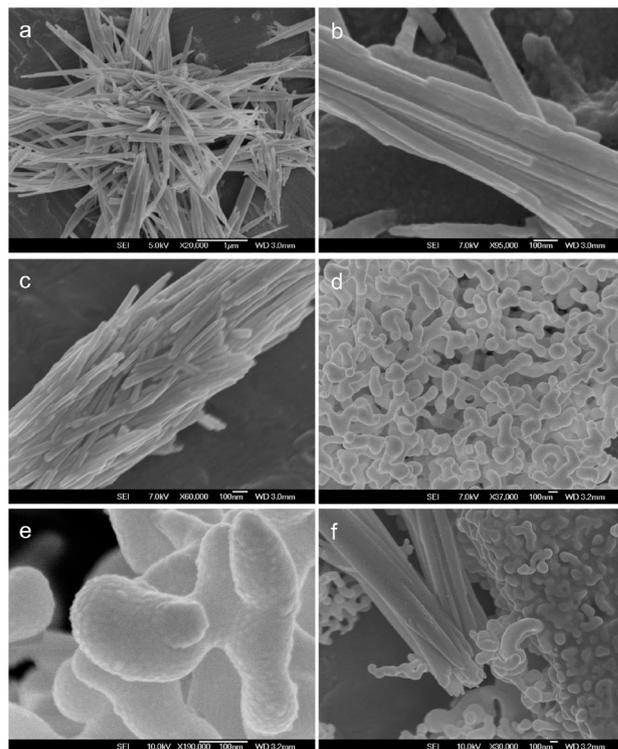

Figure 3. SEM images of SS-CdSiO$_3$ (a-c) and MS-CdSiO$_3$ (d-f).

both cases, is very different from the large aggregates seen when the conventional solid state route is used. The material SS-CdSiO$_3$ (Figure 2 a-c) is composed of needle-shaped nanoparticles which reflect the low dimensionality of the crystal structure. The individual needles are 1-4 μm long by 50-100 nm wide and can be arranged in bundles forming long wires with diameters in the micrometer range, as shown in Figure 2c. This type of morphology cannot be observed in CdSiO$_3$ prepared by the conventional high-temperature solid state reaction because the high temperatures and long heating times favor particle coalescence into irregular agglomerates. In contrast, the material MS-CdSiO$_3$ (Figure 3 d-f) shows a coralloid morphology with approximate diameters around 100 nm. The coralloid shape is an indication that CdSiO$_3$ forms initially in the spherical shape of the precursor silica particles (Figure S3). This means that molten CdCl$_2$ diffuses into the mesostructures, covering their surface and reacting to form CdSiO$_3$. The presence of elongated structures in Figure 3f suggests that heating at higher temperatures may lead to the formation of the elongated structures seen in SS-CdSiO$_3$. This morphology control may have important implications when using these materials as a matrix for long lasting phosphorescence, especially for medical applications, where the shape and size of the particles may determine their path through the human body. To check if these needle-shaped particles are nanotubes, which should be hollow, SS-CdSiO$_3$ was observed by FIB microscopy and TEM as shown in Figure 4. The FIB images (Figure 4 a-b) show that the individual nanoparticles have an approximately circular cross-section, diameters as small as 25 nm,
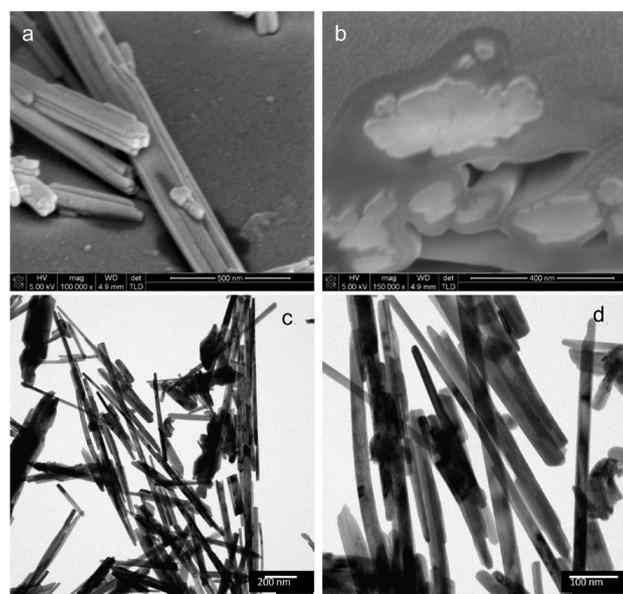
and are not hollow, which means that they are best described as nanorods. Transmission electron microscopy (Figure 4 c-d) shows that the primary nanoparticles are 500-700 nm long by 20-50 nm wide, with high aspect ratios, varying from 10:1 to 35:1.

Conclusions

CdSiO$_3$ nanostructures have been prepared at the lowest temperature and shortest reaction times known to us, using two very simple synthetic routes. The use of molten CdCl$_2$ as a reagent in a molten salt-type approach yields pure, single-phase nanorods when Na$_2$SiO$_3$ is used as the Si source, while a coralloid morphology, representing a transition from spherical to needle-like form, is observed when the Si source is high surface area mesostructured SiO$_2$. In this case, the conversion is not complete and amorphous silica is still present. This is a very promising method because it is simple, straightforward and cost-effective. The choice of an adequate precursor allows a morphology control of the resulting particles, with possible implications in medical applications.

Supplementary Information

Supplementary data are available free of charge at http://jbcs.sbq.org.br as PDF file.

Acknowledgments

Figure 4. FIB (a, b) and TEM images (c, d) of SS-CdSiO$_3$.

References

1. Chang, C. K.; Mao, D. L.; Shen, J. F.; Feng, C. I.; *J. Alloys Compd.* **2003**, *348*, 224.

2. Lin, L.; Shi, C. S.; Wang, Z. F.; Zhang, W. P.; Yin, M.; *J. Alloys Compd.* **2008**, *466*, 546.

3. Lin, L.; Yin, M.; Shi, C. S.; W. Zhang, W. P.; *J. Alloys Compd.* **2008**, *455*, 327.

4. Gary, E. N.; *A History of Luminescence*; American Philosophical Society: Philadelphia, PA, 1957, p. 18.

5. Gubelin, E.; *International World of Gemstones*; ABC-Verlag: Zurich, 1974.

6. Feldman, C.; Justel, T.; Ronda, C. R.; Schmidt, P. J.; *Adv. Funct. Mater.* **2003**, *13*, 511.

7. Green, W. H.; Lee, K. P.; Grey, J.; Au, T. T.; Sailor, M. J.; *Science* **1997**, *276*, 1826.

8. Wang, X.; Zhuang, J.; Chen, J.; Zhou, K. B.; Li, Y. D.; *Angew. Chem., Int. Ed.* **2004**, *43*, 2017.

9. Wang, X.; Zhuang, J.; Peng, Q.; Li, D.; *J. Solid State Chem.* **2005**, *178*, 2332.

10. Ferracin, L. C.; Davolos, M. R.; Nunes, L. A. O.; *J. Lumin.* **1997**, *72-74*, 185.

11. Dent, L. S.; Glasser, F. P.; *Inorg. Chem.* **1964**, *3*, 1228.

12. Barboza, C. A.; Henriques, J. M.; Albuquerque, E. L.; Caetano, E. W. S.; Freire, V. N.; da Costa, L. A. O.; *Chem. Phys. Lett.* **2009**, *480*, 273.

13. Zhang, L.; Hong, G. Y.; Sun, X. I.; *Chin. Chem. Lett.* **1999**, *10*, 799.

14. Lei, B.; Liu, Y.; Ye, Z.; Shi, C.; *Chem. Lett.* **2003**, *32*, 904.

15. Lei, B.; Liu, Y.; Ye, Z.; Shi, C.; *J. Solid State Chem.* **2004**, *177*, 1333.

16. Kuang, J.; Liu, Y.; *Chem. Phys. Lett.* **2006**, *424*, 58.

17. Liu, Y.; Lei, B.; Shi, C.; *Chem. Mater.* **2005**, *17*, 2108.

18. Liu, Y.; Kuang, J.; Lei, B.; Shi, C.; *J. Mater. Chem.* **2005**, *15*, 4025.

19. Lei, B.; Liu, Y.; Ye, Z.; Shi, C.; *J. Lumin.* **2004**, *109*, 215.

20. Parhi, P.; Manivannan, V.; *Mater. Lett.* **2008**, *62*, 3468.

21. Qu, X.; Cao, L.; Liu, W.; Su, G.; Qu, H.; Xu, C.; *J. Alloys Compd.* **2009**, *484*, 641.

22. Wang, J.; Ge, J.; Zhang, H.; Li, Y.; *Small* **2006**, *2*, 257.

23. Mao, Y.; Park, T. -J.; Zhang, F.; Zhou, H.; Wong, S. S.; *Small* **2007**, *3*, 1122.

24. Hayashi, Y.; Kimura, T.; Yamaguchi, T.; *J. Mater. Sci.* **1986**, *21*, 757.

25. Yoon, K. H.; Cho, Y. S.; Kang, D. H.; *J. Mater. Sci.* **1998**, *33*, 2977.